RSC Advances

PAPER

View Article Online
View Journal | View Issue

Cite this: *RSC Adv.*, 2022, **12**, 20088

Effective regulation of the electronic properties of a biphenylene network by hydrogenation and halogenation†

Yunhao Xie,[a] Liang Chen,[ab] Jing Xu *[a] and Wei Liu *[a]

A biphenylene network, the first synthesized non-graphene planar carbon allotrope composed entirely of sp^2-hybridized carbon atoms, has attracted widespread interest due to its unique structure, and electronic and mechanical properties. A pristine biphenylene network is metallic, and the effective regulation of its electronic properties will greatly expand its application in the fields of optoelectronics, nanoelectronic devices and photocatalysis. In this paper, the hydrogenation and halogenation of biphenylene networks were investigated using density functional theory, and their electronic properties were tuned by varying the functionalization concentration. Calculation results show that the maximum functionalization degree is $CH_{1.00}$, $CF_{1.00}$, $CCl_{0.67}$ and $CBr_{0.33}$, respectively. The band gap could be modulated in the range of 0.00–4.86 eV by hydrogenation, 0.012–4.82 eV by fluorination, 0.090–3.44 eV by chlorination, and 0.017–1.73 eV by bromination. It is also found that CH_x (x = 0.92, 1.00), CF_x (x = 0.75, 1.00), and CCl_x (x = 0.42–0.67) have the potential to photolyse water. Our research indicates that hydrogenation and halogenation can effectively regulate the electronic properties of the biphenylene network by controlling the concentration of functionalization, thus expanding its potential applications in the field of electronic devices and photocatalysis.

Received 14th June 2022
Accepted 4th July 2022

DOI: 10.1039/d2ra03673h

rsc.li/rsc-advances

Introduction

Graphene, a two-dimensional (2D) monolayer honeycomb lattice structure composed of sp^2-carbon atoms,[1] has received extensive attention due to its unique chemical and physical properties,[2–5] and has been successfully applied in the fields of energy, biology and medicine.[6–13] As a new allotrope of graphene, a biphenylene network has a different fully sp^2-hybridized carbon network composed of quadrilaterals, hexagons and octagons, and has several fascinating properties.[14–17] Owing to the existence of non-hexagonal rings, the synthesis of a biphenylene network has always been a great challenge. Until 2021, Gottfried *et al.* reported the bottom-up growth of a biphenylene network with periodically arranged quadrilaterals, hexagons and octagons of sp^2-hybridized carbon atoms through an on-face inter-polymer dehydrofluorination reaction.[18] This was the successful synthesis of the first non-graphene planar carbon allotropes composed entirely of sp^2-carbon atoms.

The biphenylene network has exhibited strong lithium and sodium storage capabilities,[19,20] which reveals its great potential as an anode material. However, the metallicity of the biphenylene network[16] limits its potential application in the field of optoelectronics, electronic devices and photocatalysis. Numerous previous studies have reported that the conversion of sp^2-C atoms into sp^3-C atoms by functionalization is an effective way to regulate the electronic properties of graphene and other 2D carbon allotropes.[21–24] For example, Gao *et al.*[21] modulated the band gap of graphene in the range of 0.00–4.66 eV by changing the degree of hydrogenation. Subsequently, nearly fully hydrogenated graphene was successfully synthesized[25] and showed great application potential in the fields of electrocatalysis, photocatalysis, flexible spintronic devices and photodetectors.[26–29] Similarly, halogenated graphene can be used as catalysts for redox reactions and as hydrophobic materials due to its non-zero band gap.[30,31] Hydrogenation and halogenation are also used to successfully modulate the band gaps of graphene allotropes by varying the concentrations of functionalization. Our previous work found that the band gap of graphenylene can be regulated in a wide range by hydrogenation and halogenation, and the modified graphenylenes at some concentrations can be used as potential materials for water photolysis.[32] Inspired by these works, we believe that chemical functionalization is expected to be an effective way to regulate the electronic properties of biphenylene network, thus expanding its application potential. Up to now, the band gap of

[a]*Department of Optical Engineering, College of Optical, Mechanical and Electrical Engineering, Zhejiang A&F University, Hangzhou, Zhejiang, 311300, P. R. China. E-mail: weiliu@zafu.edu.cn; jingxu@zafu.edu.cn*

[b]*School of Physical Science and Technology, Ningbo University, Ningbo, Zhejiang, 315211, P. R. China*

† Electronic supplementary information (ESI) available. See https://doi.org/10.1039/d2ra03673h

fully hydrogenated biphenylene network up to 4.00 eV (ref. 33 and 34) and the insulating properties of fully hydrogenated biphenylene network nanoribbons[35] all demonstrate that the electronic properties of biphenylene network can be tuned effectively by functionalization. Hence, it is of great significance to systematically investigate the functionalization of biphenylene network and explore the regulation of electronic properties under different functionalization degrees.

In this work, biphenylene networks were hydrogenated and halogenated at 12 different concentrations, and the structures, stabilities and electronic properties of the obtained functionalized biphenylene networks were investigated using first-principles calculations. The results show that by controlling the concentrations of hydrogenation and halogenation, the band gap of functionalized biphenylene networks can be adjusted in a wide range, *i.e.*, 0.00–4.86 eV for hydrogenation and 0.012–4.82 eV for halogenation. The fluorinated biphenylene network has the highest thermodynamic stability. The band-edge calculations show that some functionalized biphenylene networks are feasible as catalysts for water photolysis. Our work shows that the electronic properties of biphenylene network can be successfully regulated by hydrogenation and halogenation with different concentrations, thus expanding its potential application in 2D electronic devices and photocatalysis.

Methodology

All calculations in this work were carried out by density functional theory (DFT)[36] as implemented in Vienna *ab initio* simulation package (VASP)[37] with a projector augmented wave (PAW)[38] method. The generalized gradient approximation (GGA) with Perdew–Burke–Ernzerhof (PBE)[39] scheme was used to describe the exchange correlation energy functional. Due to the underestimation of the band gap by PBE, the Heyd–Scuseria–Ernzerhof (HSE)[40] scheme was also used to obtain accurate band gap values. To avoid the interaction between two neighboring slabs, the vacuum thickness was set to 20 Å along the *z*-direction. The plane wave cutoff energy was taken to be 550 eV in all calculations. The Brillouin zone was sampled by 3 × 3 × 1 Monkhorst–Pack[41] *k*-points mesh. The convergence criteria for energy and Hellmann–Feynman force were set to 10^{-5} eV per atom and 10^{-2} eV $Å^{-1}$ during the geometric optimization, respectively.

Results and discussion

Fig. 1a shows the optimized structure of biphenylene network in a 2 × 2 supercell consisting of four quadrilaterals, four hexagons and four octagons. It contains a total of 24 sp^2-hybridized C atoms, which form four types of C–C bonds with bond lengths of 1.41 Å, 1.45 Å, 1.45 Å and 1.46 Å, respectively. The lattice parameters of the optimized biphenylene network are $a = 7.51$ Å and $b = 9.05$ Å. These geometric parameters are consistent with previously reported work.[42] In this work, we systematically study hydrogenated and halogenated biphenylene networks at different concentrations. The obtained functionalized

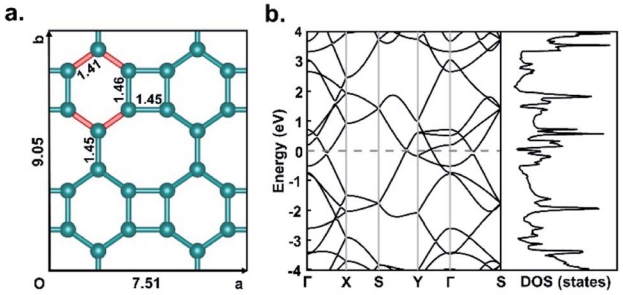

Fig. 1 (a) Top view of the 2D structure of biphenylene network in a 2 × 2 supercell. The unit of lattice parameters and bond lengths is angstrom (Å). (b) The PBE band structures and density of states of biphenylene network.

biphenylene networks were named as CM_x, where M is the functionalization atom (including hydrogen, fluorine, chlorine, bromine and iodine), and x is the concentration of functionalization. Totally 12 hydrogen or halogen molecules can be adsorbed on the surface of a biphenylene network 2 × 2 supercell, therefore there are 12 concentration values, *i.e.*, x = 0.08, 0.17, 0.25, 0.33, 0.42, 0.50, 0.58, 0.67, 0.75, 0.83, 0.92, 1.00.

Among the four types of C–C bonds, the bond shared by hexagon and octagon (highlighted in red in Fig. 1a) has the shortest bond length, which indicates that it has more double bond nature. Therefore, in the process of functionalization, the first pair of M atoms were preferentially adsorbed on this C–C bond, with one atom above the biphenylene network plane and the other below the plane. It is worthy to note that combining M atoms on different sides of biphenylene network to form sp^3-C can increase the distance between the atoms on the same side, reduce interactions and avoid aggregation, thus making the whole structure more stable. With the increase of the functionalization concentration, more pairs of M atoms will be adsorbed on the surface of biphenylene network. We considered all possible adsorption positions and only selected the energetically most stable structures for further investigations. Fig. 2 summarizes the binding order of M atoms on the surface of biphenylene network. It can be seen that hydrogen and fluorine atoms are preferentially bound to the same hexagon until this ring is fully functionalized before being added to other hexagons. The difference is that the second hexagon for hydrogenation is connected to the first hexagon through a quadrilateral, while the second hexagon for fluorination is connected to the first hexagon through an octagon. Chlorine and bromine atoms are gradually added to different hexagons, which could be attributed to their larger atomic radii.

The most stable structures of hydrogenated, fluorinated, chlorinated, and brominated biphenylene networks at different concentrations are shown in Fig. 3a–d and S1a–d.† It should be noted that we did not obtain any stable configuration for the addition of iodine to biphenylene network, so the iodination of biphenylene network is impossible. As seen from Fig. 3, hydrogenated and fluorinated biphenylene networks at 12 concentrations can be obtained, while the maximum concentrations of chlorination and bromination are only 0.67 and 0.33.

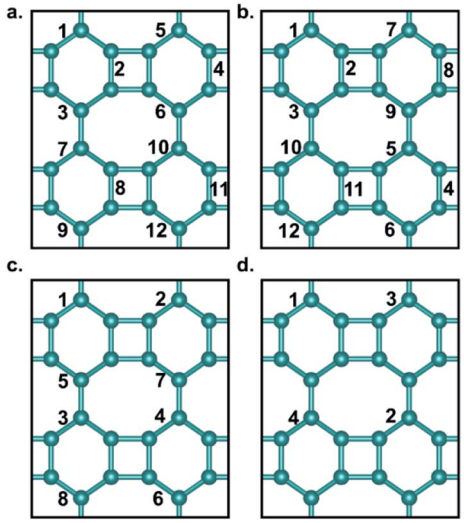

Fig. 2 The binding order of H (a), F (b), Cl (c) and Br (d) atoms to biphenylene network.

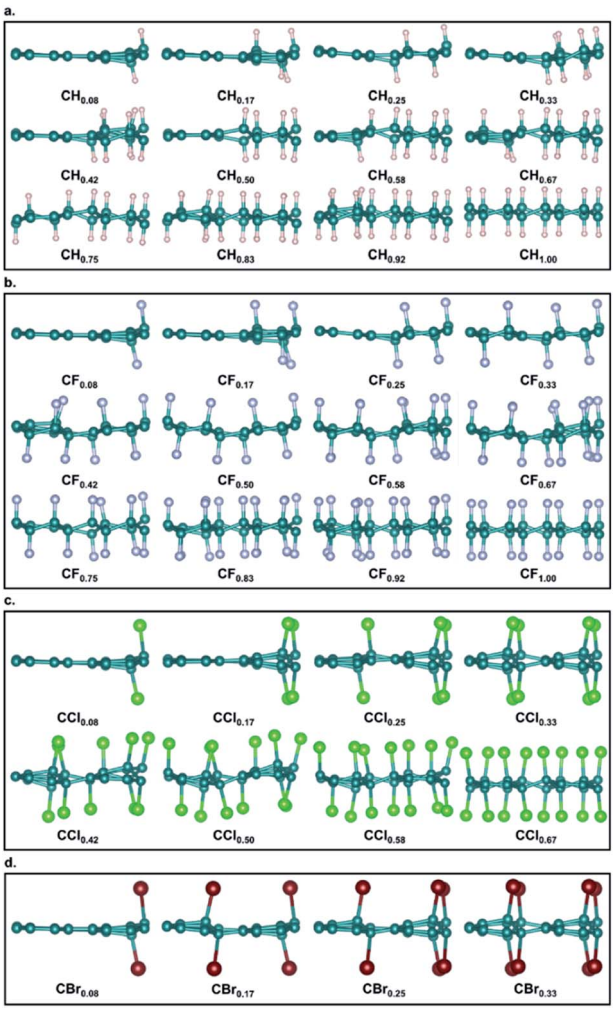

Fig. 3 The side views of structures of biphenylene networks functionalized by H (a), F (b), Cl (c) and Br (d) at different concentrations.

Comparing the structures of all the functionalized biphenylene networks, it can be found that the structures gradually become plicated, which is because sp^3-hybridized C atoms become dominant with increasing the concentration of functionalization.

The lattice parameters of the functionalized biphenylene network structures are shown in Table 1. For hydrogenation, fluorination, and chlorination, the lattice parameters in the a and b directions change very slightly at low concentrations, and then increase with the increase of concentrations, which is 3% and 2% for hydrogenation, 6% and 5% for fluorination and 5% and 8% for chlorination. For bromination, the lattice parameters of brominated biphenylene networks are almost unchanged because the maximum concentration of bromination is only 0.33.

In order to investigate the thermodynamic stability of functionalized biphenylene networks and the effect of different concentrations of M atoms on the thermodynamic stability, we calculated the binding energies for the most stable structures in each system. The calculation formula is as follows:

$$E_{\text{binding}}{}^{x}\,(\text{M}) = (E_{\text{CM}_x} - E_{\text{biphenylene network}} - nE_{\text{M}})/n$$

where $E_{\text{binding}}{}^{x}$ (M) is the binding energy of each M atom at functionalization concentration x, E_{CM_x} is the total energy of functionalized biphenylene network CM_x, $E_{\text{biphenylene network}}$ is the energy of the pristine biphenylene network, E_{M} is the energy of per M atom of an M_2 molecule in vacuum, and n is the number of M atoms in a functionalized biphenylene network. All calculated binding energies are plotted in Fig. 4. As can be seen from the figure, the binding energies of hydrogen and fluorine atoms are always negative at all concentrations, ranging from −0.43 to −0.070 eV per atom for hydrogenation and −1.92 to −1.78 eV per atom for fluorination. With the increase of concentration, the binding energies of hydrogen atoms decrease slightly, while those of fluorine atoms remain almost unchanged. For the chlorinated biphenylene networks, the binding energies are negative (−0.13 to −0.070 eV per atom) at concentrations below 0.33, but become positive and gradually increase with increasing concentrations. For brominated biphenylene networks, the binding energies are always positive. These positive binding energies indicate that the binding of bromine atoms on biphenylene network is endothermic and therefore unstable. The fluorine atom has the lowest binding energy among the four atoms, which can be attributed to the strongest electronegativity and smaller ionic radius of fluorine. The gradually decreasing binding energy of chlorine and bromine atoms to biphenylene network is owning to their larger atomic radius and mutual repulsion.

Generally, different methods of hydrogenation and halogenation will have different effects on the stability of functionalized biphenylene networks. In our work, we considered a variety of possible ways of adding M atoms, and finally found that the structures with preferentially addition of M atoms to the hexagons on both sides of biphenylene network have the best stability. Compared with the work of hydrogenated biphenylene network reported by Lee *et al.*,[34] the binding energy of each H

Table 1 The lattice parameters (Å) of hydrogenated and halogenated biphenylene networks at different concentrations

	Hydrogenation		Fluorination		Chlorination		Bromination	
Concentration	*a*	*b*	*a*	*b*	*a*	*b*	*a*	*b*
0.08	7.51	9.05	7.51	9.04	7.51	9.05	7.51	9.05
0.17	7.55	9.04	7.54	9.04	7.51	9.03	7.51	9.03
0.25	7.59	9.04	7.61	9.04	7.49	9.03	7.50	9.03
0.33	7.58	9.06	7.65	9.05	7.49	9.01	7.50	9.02
0.42	7.58	9.10	7.67	9.05	7.56	9.15		
0.50	7.61	9.13	7.75	9.06	7.61	9.28		
0.58	7.61	9.15	7.77	9.14	7.76	9.53		
0.67	7.67	9.13	7.78	9.18	7.91	9.87		
0.75	7.70	9.16	7.83	9.26				
0.83	7.70	9.19	7.86	9.34				
0.92	7.70	9.21	7.88	9.41				
1.00	7.73	9.25	7.94	9.49				

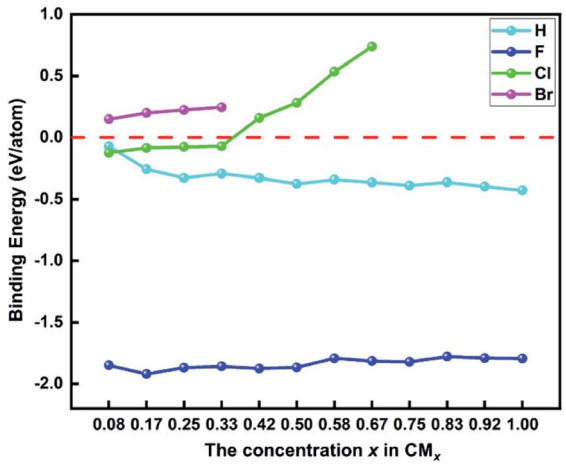

Fig. 4 The binding energies of hydrogen and halogen atoms on biphenylene networks at different concentrations.

atom is −0.36 eV at the concentration of 1.00, which is higher than ours (−0.43 eV per H). Clearly, the fully hydrogenated biphenylene network obtained in this work has better thermodynamic stability, which is mainly due to different hydrogenation methods. In their work, hydrogen is preferentially added to quadrilaterals on the same side, and the mutual repulsion of these hydrogen atoms may reduce the binding stability to the substrate. Therefore, the hydrogenation method proposed by us is a more suitable and effective method for hydrogenating biphenylene network, and this strategy can be applied to the research of other functionalized materials in the future.

In order to explore the effect of functionalization on the electronic properties, we calculated the electronic band structures and densities of states of pristine and functionalized biphenylene networks. As shown in Fig. 1b, the pristine biphenylene network has a zero-band gap and exists states near the Fermi level, indicating its metallicity, which is consistent with previous reports.[16] The PBE band structures and densities of states of hydrogenated biphenylene networks at different concentrations are shown in black lines in Fig. 5. Due to the well-known underestimation of the band gaps by PBE function, a hybrid DFT functional (HSE)[40] was used to obtain more accurate band gap values, as shown in red lines in Fig. 5. Note that the following discussions of band gaps are all based on HSE results. The band gap results show that for CH_x, when x is 0.08–0.50, the band gaps are 0.21, 0.14, 0.066, 0.00, 0.13 and 0.11 eV, respectively. Hydrogenated biphenylene networks are metallic at 0.33 and semiconducting with small indirect band gaps at all other concentrations. When x is 0.58–1.00, the band gaps are opened to 1.05, 3.69, 4.53, 3.90, 4.86, and 4.82 eV, respectively. They have direct band gaps at the concentration of 0.67 and 0.75, and indirect band gaps at other concentrations. The bands near the valence band maximum (VBM) and conduction band minimum (CBM) have great dispersion effects when $x \leq 0.50$, which reflects high mobilities of electrons and holes. However, when $x > 0.50$, the bands near VBM and CBM gradually become flatter, which indicates that the mobilities of electrons and holes decrease gradually.

The PBE and HSE band structures and densities of states of halogenated biphenylene networks at different concentrations are shown in Fig. S2–S4.† For CF_x, there is the similar trend with hydrogenation. At low concentrations, fluorinated biphenylene networks are semiconductors with indirect small band gaps (0.097, 0.014 and 0.012 eV), and with the increase of concentrations, the band gaps are opened to 1.81, 3.13, 4.14, 3.81, 4.40, 4.56, 3.89, 4.68, 4.82 eV when $x > 0.33$. Among which, they have direct band gaps when x is 0.50, 0.67, 0.75 and 0.83, and indirect band gaps at other concentrations. Unlike hydrogenation, the bands near the Fermi level become flat when x is 0.33. For CCl_x, small indirect band gaps (0.15 and 0.090 eV) were obtained when x is 0.08 and 0.17 and the band gaps were opened to 1.00, 2.24, 2.16, 2.55, 2.56 and 3.44 eV at the concentrations of 0.25–0.67. Except $x = 0.50$ and 0.67, all the chlorinated biphenylene networks have direct band gaps. For CBr_x, the band gaps are 0.13, 0.017, 0.97, and 1.73 eV, respectively, and there exists only one direct band gap ($x = 0.25$). For both chlorination and bromination, the bands near the Fermi level become flat at $x = 0.25$, which is earlier than other three systems.

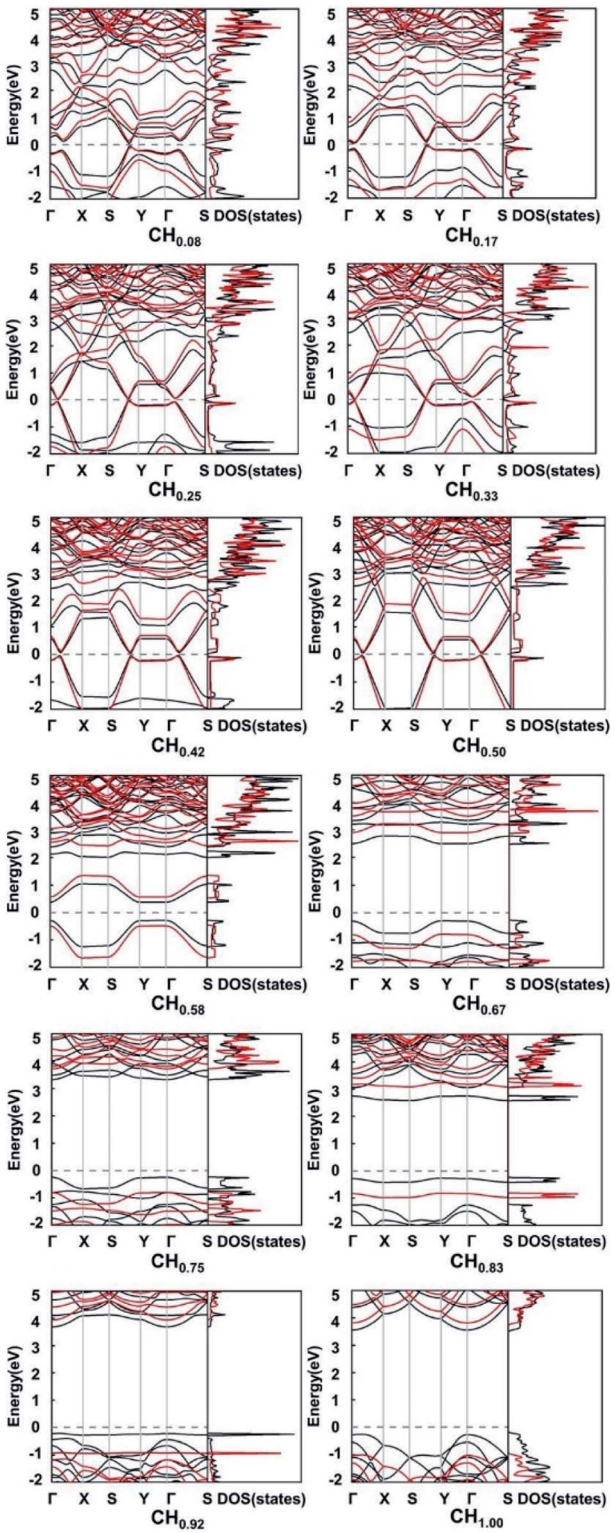

Fig. 5 The PBE (black lines) and HSE (red lines) band structures of hydrogenated biphenylene networks at different hydrogen concentration x. The Fermi levels are shown by dashed lines.

Fig. 6 summarizes the calculated PBE and HSE band gaps of hydrogenated and halogenated biphenylene networks as the function of concentration x. It can be seen from the figure that the variation trend of the changes of two kinds of band gaps with concentrations is consistent, but the HSE band gaps are always larger than the PBE values at the same functionalization concentration. For example, for hydrogenated biphenylene network at $x = 1.00$, the PBE band gap is 3.82 eV, which is 1 eV smaller than 4.82 eV calculated by HSE. The band gaps are maintained in a narrow range before $CH_{0.50}$, $CF_{0.25}$, $CCl_{0.17}$, and $CBr_{0.17}$. Then the band gaps gradually increase with the increases of concentrations, and reach the maximum values at $CH_{0.92}$, $CF_{1.00}$, $CCl_{0.67}$, and $CBr_{0.33}$. Based on the above discussion, functionalization can tune the band gaps of biphenylene networks over a wide range, and the tuning range is 0.00–4.86 eV for hydrogenation, 0.012–4.82 eV for fluorination, 0.090–3.44 eV for chlorination, and 0.017–1.73 eV for bromination, respectively.

To investigate the potential applications of functionalized biphenylene networks for photolysis of water, we also performed band-edge calculations at different concentrations and aligned the band edges with the normal hydrogen electrode (NHE) potential. The vacuum energy levels of each structure were obtained by calculating their electrostatic potentials using VASPKIT[45] and their VBM and CBM were firstly aligned with the vacuum energy levels. Then, the corresponding VBM and CBM relative to NHE are calculated using the following formula:

$$E_{NHE} = -4.5 - E_{vac}/e$$

where E_{NHE} and E_{vac} are the values of VBM and CBM relative to NHE and the energy levels of vacuum, respectively. The calculated VBM and CBM positions using the PBE and HSE functionals are plotted in Fig. 7, and the dashed lines in the figure represent the redox potentials of photolysis of water. As seen from Fig. 7, VBM and CBM of halogenated biphenylene networks are lower than those of hydrogenated biphenylene networks at the same functionalization concentration, which indicates that halogenated biphenylene networks have larger ionization energies and electron affinities. It is known that when VBM is lower than the potential of OER oxidation reaction and CBM is higher than the potential of HER reduction reaction, it can be a potential semiconductor material for photolysis of water.[43] It can be seen from the figure that the band-edge energies of $CH_{0.92}$, $CH_{1.00}$, $CF_{0.75}$, $CF_{1.00}$, $CCl_{0.42}$, $CCl_{0.50}$, $CCl_{0.58}$ and $CCl_{0.67}$ completely cover the redox potentials for photolysis of water. Their CBMs are 3.58, 3.55, 0.028, 0.20, 0.21, 0.45, 0.97, and 1.62 eV higher than the HER potentials, and VBMs are 0.049, 0.034, 3.30, 3.39, 0.72, 0.86, 0.35, and 0.59 eV lower than the OER potentials, respectively. Previous study has demonstrated that the larger energy difference between CBM/VBM and the water reduction/oxidation potential, the higher reducing/oxidizing ability.[44] Therefore, $CH_{0.92}$ has the strongest reduction ability, and $CF_{1.00}$ has the strongest oxidation ability. For other functionalized biphenylene networks, CH_x (x = 0.67–0.83) possess favorable CBM positions for HER to produce hydrogen, while CF_x (x = 0.33–0.67, 0.83 and 0.92), CCl_x and CBr_x (x = 0.25 and 0.33) have suitable positions for OER to produce oxygen. In summary, functionalized biphenylene networks show their potential in catalytic applications by modulating the concentrations of hydrogenation and halogenation.

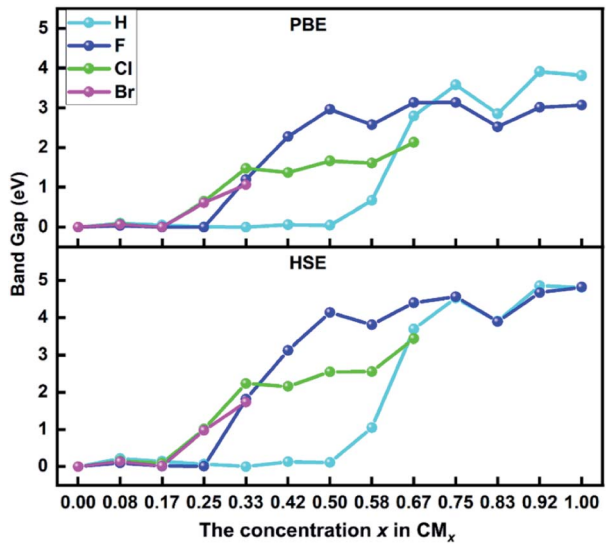

Fig. 6 The calculated PBE and HSE band gap values of biphenylene networks functionalized by hydrogen and halogen atoms as a function of the concentration *x*.

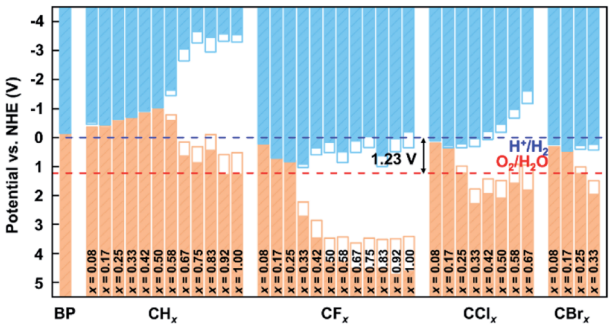

Fig. 7 Band edges of biphenylene network and functionalized biphenylene networks relative to NHE. The blue and orange lines represent the PBE results, while the columns filled by blue and orange colors represent the HSE results. The dashed lines indicated the water redox potentials.

Conclusions

In this work, we explored the hydrogenation and halogenation of biphenylene networks using first-principles calculations, and modulated the electronic properties by varying the concentration of functionalization. The calculation results show that the maximum functionalization concentrations are 1.00 for hydrogenation and fluorination, 0.67 for chlorination and 0.33 for bromination, respectively. Among functionalized biphenylene networks, fluorinated biphenylene networks possess the best thermodynamic stabilities. Calculations of the electronic properties show that the band gaps of biphenylene network were opened very weakly at low concentrations of functionalization, and could be modulated over a wide range with increasing the concentrations. The band gaps can be regulated in the range of 0–4.86 eV for hydrogenation, 0.012–4.82 eV for fluorination, 0.090–3.44 eV for chlorination, and 0.017–1.73 eV for bromination, respectively. The band-edge calculations show that the functionalized biphenylene networks have catalytic potential for photolysis of water at the concentrations of 0.92 and 1.00 for hydrogenation, 0.75 and 1.00 for fluorination, and 0.42–0.67 for chlorination. Our work illustrates that hydrogenation and halogenation can effectively modulate the electronic properties of biphenylene networks, which may have potential applications in electronic devices, photocatalysis and other fields.

Author contributions

W. L., Y. X. and J. X. conceived the research; Y. X. and W. L. performed the calculations and analyzed the data; W. L., Y. X. and J. X. wrote the manuscript; L. C. helped to revise the manuscript. All authors discussed and commented on the manuscript.

Conflicts of interest

There are no conflicts to declare.

Acknowledgements

This work is supported by the National Natural Science Foundation of China (No. 11975206, 12075211, U1832150), the Natural Science Foundation of Zhejiang Province (No. LQ20B030002), the Scientific Research Foundation of Zhejiang A&F University (No. 2019FR005, 2019FR006).

Notes and references

1 M. Terrones, A. R. Botello-Méndez, J. Campos-Delgado, F. López-Urías, Y. I. Vega-Cantú, F. J. Rodríguez-Macías, A. L. Elías, E. Muñoz-Sandoval, A. G. Cano-Márquez and J.-C. Charlier, Graphene and graphite nanoribbons: Morphology, properties, synthesis, defects and applications, *Nano Today*, 2010, **5**, 351–372.
2 M. J. Allen, V. C. Tung and R. B. Kaner, Honeycomb Carbon: A Review of Graphene, *Chem. Rev.*, 2010, **110**, 132–145.
3 A. H. Castro Neto, F. Guinea, N. M. R. Peres, K. S. Novoselov and A. K. Geim, The electronic properties of graphene, *Rev. Mod. Phys.*, 2009, **81**, 109–162.
4 K. Wakabayashi, Physical properties of nano-graphene, *Carbon*, 2010, **48**, 4216.
5 D. G. Papageorgiou, I. A. Kinloch and R. J. Young, Mechanical properties of graphene and graphene-based nanocomposites, *Prog. Mater. Sci.*, 2017, **90**, 75–127.
6 S. Guo and S. Dong, Graphene nanosheet: synthesis, molecular engineering, thin film, hybrids, and energy and analytical applications, *Chem. Soc. Rev.*, 2011, **40**, 2644.
7 Y. Sun, Q. Wu and G. Shi, Graphene based new energy materials, *Energy Environ. Sci.*, 2011, **4**, 1113.
8 F. Perreault, A. Fonseca de Faria and M. Elimelech, Environmental applications of graphene-based nanomaterials, *Chem. Soc. Rev.*, 2015, **44**, 5861–5896.

9 V. Georgakilas, J. N. Tiwari, K. C. Kemp, J. A. Perman, A. B. Bourlinos, K. S. Kim and R. Zboril, Noncovalent Functionalization of Graphene and Graphene Oxide for Energy Materials, Biosensing, Catalytic, and Biomedical Applications, *Chem. Rev.*, 2016, **116**, 5464–5519.

10 C. Cheng, S. Li, A. Thomas, N. A. Kotov and R. Haag, Functional Graphene Nanomaterials Based Architectures: Biointeractions, Fabrications, and Emerging Biological Applications, *Chem. Rev.*, 2017, **117**, 1826–1914.

11 J. A. Lochala, H. Zhang, Y. Wang, O. Okolo, X. Li and J. Xiao, Practical Challenges in Employing Graphene for Lithium-Ion Batteries and Beyond, *Small Methods*, 2017, **1**, 1700099.

12 G. Reina, J. M. González-Domínguez, A. Criado, E. Vázquez, A. Bianco and M. Prato, Promises, facts and challenges for graphene in biomedical applications, *Chem. Soc. Rev.*, 2017, **46**, 4400–4416.

13 J. Han, I. Johnson and M. Chen, 3D Continuously Porous Graphene for Energy Applications, *Adv. Mater.*, 2022, **34**, 2108750.

14 Y. Luo, C. Ren, Y. Xu, J. Yu, S. Wang and M. Sun, A first principles investigation on the structural, mechanical, electronic, and catalytic properties of biphenylene, *Sci. Rep.*, 2021, **11**, 19008.

15 Q. Wang and Q. Zhou, Electronic and optical properties of biphenylene under pressure: first-principles calculations, *Mol. Simul.*, 2020, **46**, 987–993.

16 M. A. Hudspeth, B. W. Whitman, V. Barone and J. E. Peralta, Electronic Properties of the Biphenylene Sheet and Its One-Dimensional Derivatives, *ACS Nano*, 2010, **4**, 4565–4570.

17 Y.-W. Son, H. Jin and S. Kim, Magnetic Ordering, Anomalous Lifshitz Transition, and Topological Grain Boundaries in Two-Dimensional Biphenylene Network, *Nano Lett.*, 2022, **22**, 3112–3117.

18 Q. Fan, L. Yan, M. W. Tripp, O. Krejčí, S. Dimosthenous, S. R. Kachel, M. Chen, A. S. Foster, U. Koert, P. Liljeroth and J. M. Gottfried, Biphenylene network: A nonbenzenoid carbon allotrope, *Science*, 2021, **372**, 852–856.

19 T. Han, Y. Liu, X. Lv and F. Li, Biphenylene Monolayer: A Novel Nonbenzenoid Carbon allotrope with Potential Applications as Anode Materials for High-performance Sodium Ion Batteries, *Phys. Chem. Chem. Phys.*, 2022, **24**, 10712–10716.

20 Y. Kim, J. Jung, H. Yu, G. Kim, D. Jeong, D. Bresser, S. J. Kang, Y. Kim and S. Passerini, Sodium Biphenyl as Anolyte for Sodium–Seawater Batteries, *Adv. Funct. Mater.*, 2020, **30**, 2001249.

21 H. Gao, L. Wang, J. Zhao, F. Ding and J. Lu, Band Gap Tuning of Hydrogenated Graphene: H Coverage and Configuration Dependence, *J. Phys. Chem. C*, 2011, **115**, 3236–3242.

22 J. Koo, B. Huang, H. Lee, G. Kim, J. Nam, Y. Kwon and H. Lee, Tailoring the Electronic Band Gap of Graphyne, *J. Phys. Chem. C*, 2014, **118**, 2463–2468.

23 J. Koo, M. Park, S. Hwang, B. Huang, B. Jang, Y. Kwon and H. Lee, Widely tunable band gaps of graphdiyne: an ab initio study, *Phys. Chem. Chem. Phys.*, 2014, **16**, 8935–8939.

24 Y. Wang, N. Song, T. Zhang, Y. Zheng, H. Gao, K. Xu and J. Wang, Tuning the electronic and magnetic properties of graphyne by hydrogenation, *Appl. Surf. Sci.*, 2018, **452**, 181–189.

25 A. Y. S. Eng, Z. Sofer, D. Bouša, D. Sedmidubský, Š. Huber and M. Pumera, Near-Stoichiometric Bulk Graphane from Halogenated Graphenes (X = Cl/Br/I) by the Birch Reduction for High Density Energy Storage, *Adv. Funct. Mater.*, 2017, **27**, 1605797.

26 X. Han, X. Tong, X. Liu, A. Chen, X. Wen, N. Yang and X.-Y. Guo, Hydrogen Evolution Reaction on Hybrid Catalysts of Vertical MoS_2 Nanosheets and Hydrogenated Graphene, *ACS Catal.*, 2018, **8**, 1828–1836.

27 A. H. Reshak, Chairlike and Boatlike Graphane: Active Photocatalytic Water Splitting Solar-to-Hydrogen Energy Conversion under UV Irradiation, *J. Phys. Chem. C*, 2018, **122**, 8076–8081.

28 L. Zhang, F. Zhai, K.-H. Jin, B. Cui, B. Huang, Z. Wang, J. Lu and F. Liu, Quantum Spin Hall Effect and Tunable Spin Transport in As-Graphane, *Nano Lett.*, 2017, **17**(7), 4359–4364.

29 P. Gowda, D. R. Mohapatra and A. Misra, Enhanced Photoresponse in Monolayer Hydrogenated Graphene Photodetector, *ACS Appl. Mater. Interfaces*, 2014, **6**, 16763–16768.

30 K.-H. Wu, D.-W. Wang, Q. Zeng, Y. Li and I. R. Gentle, Solution phase synthesis of halogenated graphene and the electrocatalytic activity for oxygen reduction reaction, *Chin. J. Catal.*, 2014, **35**, 884–890.

31 K. Ibrahim, A. Shahin, A. Jones, A. H. Alshehri, K. Mistry, M. D. Singh, F. Ye, J. Sanderson, M. Yavuz and K. P. Musselman, Humidity-resistant perovskite solar cells via the incorporation of halogenated graphene particles, *Sol. Energy*, 2021, **224**, 787–797.

32 W. Liu, M. Miao and J. Liu, Band gap engineering of graphenylene by hydrogenation and halogenation: a density functional theory study, *RSC Adv.*, 2015, **5**, 70766–70771.

33 Y. Liao, X. Shi, T. Ouyang, J. Li, C. Zhang, C. Tang, C. He and J. Zhong, New Two-Dimensional Wide Band Gap Hydrocarbon Insulator by Hydrogenation of a Biphenylene Sheet, *J. Phys. Chem. Lett.*, 2021, **12**, 8889–8896.

34 S. Lee, A. Singh and H. Lee, Band gap engineering of 2D biphenylene carbon sheets with hydrogenation, *J. Korean Phys. Soc.*, 2021, **79**, 846–850.

35 P. A. Denis, Stability and Electronic Properties of Biphenylene Based Functionalized Nanoribbons and Sheets, *J. Phys. Chem. C*, 2014, **118**, 24976–24982.

36 W. Kohn and L. J. Sham, Self-Consistent Equations Including Exchange and Correlation Effects, *Phys. Rev.*, 1965, **140**, A1133–A1138.

37 G. Kresse and J. Furthmüller, Efficient iterative schemes for *ab initio* total-energy calculations using a plane-wave basis set, *Phys. Rev. B: Condens. Matter Mater. Phys.*, 1996, **54**, 11169–11186.

38 G. Kresse and D. Joubert, From ultrasoft pseudopotentials to the projector augmented-wave method, *Phys. Rev. B: Condens. Matter Mater. Phys.*, 1999, **59**, 1758–1775.

39 J. P. Perdew, K. Burke and M. Ernzerhof, Generalized Gradient Approximation Made Simple, *Phys. Rev. Lett.*, 1996, **77**, 3865–3868.
40 J. Heyd, G. E. Scuseria and M. Ernzerhof, Hybrid functionals based on a screened Coulomb potential, *J. Chem. Phys.*, 2003, **118**, 8207–8215.
41 H. J. Monkhorst and J. D. Pack, Special points for Brillouin-zone integrations, *Phys. Rev. B: Solid State*, 1976, **13**, 5188–5192.
42 H. Shen, R. Yang, K. Xie, Z. Yu, Y. Zheng, R. Zhang, L. Chen, B.-R. Wu, W.-S. Su and S. Wang, Electronic and optical properties of hydrogen-terminated biphenylene nanoribbons: a first-principles study, *Phys. Chem. Chem. Phys.*, 2022, **24**, 357–365.
43 J. R. Bolton, S. J. Strickler and J. S. Connolly, Limiting and realizable efficiencies of solar photolysis of water, *Nature*, 1985, **316**, 495–500.
44 X. Jiang, P. Wang and J. Zhao, 2D covalent triazine framework: a new class of organic photocatalyst for water splitting, *J. Mater. Chem. A*, 2015, **3**, 7750–7758.
45 V. Wang, N. Xu, J.-C. Liu, G. Tang and W.-T. Geng, VASPKIT: A user-friendly interface facilitating high-throughput computing and analysis using VASP code, *Comput. Phys. Commun.*, 2021, **267**, 108033.